RESEARCH ARTICLE

Synthesis, Characterization, Biological Activity and Thermal Study of New Complexes [Ni II, Hg II and La III] from Mixed Ligands (Curcumin and Azo compounds type N_2O_2)

Muna A. Shakir[1], Wurood A. Jaafar[2]*, Malath K. Rasheed[3]

[1]*Taiba High School for Girls, Al-Karkh/3 Education Directorate.*
[2]*Department of Chemistry, College of Education for Pure Sciences (Ibn Al-Haitham), University of Baghdad, Iraq.*
[3]*Department of Chemistry, College of Education, University of Samarra, Iraq.*

Received: 04th April, 2022; Revised: 14th July, 2023; Accepted: 18th August, 2023; Available Online: 25th September, 2023

ABSTRACT

The compound [L] was produced in the current study through the reaction of 4-aminoacetophenon with 4-methoxyaniline in the cold, concentrated HCl with 10% $NaNO^2$. Curcumin, several transition metal complexes (Ni (II), La (III), and Hg (II)), and compound [L] were combined in EtOH to create new complexes. UV-vis spectroscopy, FTIR, AA, TGA-DSC, conductivity, chloride content, and elemental analysis (CHNS) were used to describe the structure of produced complexes. Biological activities against fungi, *S. aureus* (G+), *Pseudomonas* (G-), *E. coli* (G-), and *Proteus* (G-) were demonstrated using complexes. Depending on the outcomes of the aforementioned methods, octahedral formulas were given as the geometrical structures for each created complex.

Keywords: Azo compound, Curcumin, 4-methoxyaniline, Complexes.

International Journal of Drug Delivery Technology (2023); DOI: 10.25258/ijddt.13.3.42

How to cite this article: Shakir MA, Jaafar WA, Rasheed MK. Synthesis, Characterization, Biological Activity and Thermal Study of New Complexes [Ni II, Hg II and La III] from Mixed Ligands (Curcumin and Azo compounds type N_2O_2). International Journal of Drug Delivery Technology. 2023;13(3):1024-1029.

Source of support: Nil.

Conflict of interest: None

INTRODUCTION

Azo compounds and their metal complexes are utilized extensively as corrosion inhibitors in the industry and in medicine as anti-oxidant, antimicrobial and anti-inflammatory agents.[1-5] Numerous organic compounds with hetero-atoms like the nitrogen, oxygen, phosphorous, and sulphur and π-electrons in triple bonds or conjugated double bonds have been studied as metal corrosion inhibitors.[6,7] Many of these, including methoxyanilin, acetophenone, and curcumin, were listed as corrosion inhibitors and were discovered to have effective corrosion inhibition properties.[8-10] The effectiveness of the inhibitors raises in a range of the O<N<S<P. It depends upon a variety of factors, including a number of active adsorption centers that are present in a molecule, its size, its charge densities, the manner of adsorption, and metallic complexes' formation.[11-14] The capacity of Schiff base ligands to create stable, densely packed complexes in the area of metal ion coordination introduces a new class of compounds for corrosion prevention. The presence of >C=N- groups causes the Schiff bases to become adsorbed on the metals' surface. Due to acting as a significant corrosion inhibitor, this adsorption characteristic causes a monolayer to spontaneously grow on the metal's surface.[15-17]

MATERIALS AND METHODS

Materials

Merck and BDH have provided all chemicals.

Instrumentation

FTIR spectra were captured with a KBr disk and a Shimadzu 8400 in the 400 to 4,000 cm^{-1} range. The TGA-DSC thermal analysis was examined and characterized. CHNS was conducted on Elemental from EuroEA.

Compound Preparation

Syntheses of 1-(4-((2-amino-5-methoxyphenyl) diazenyl) phenyl) ethan-1-one

4-Aminoacetophenone (0.002 mol) was combined with (10 mL) distilled water, (10 mL) ethanol, and (2 mL) HCl in a flask with a round bottom, and the mix was cooled to 0 to 5ºC for 30 minutes. The mixture is after added gradually while being constantly stirred to generate 4-methoxyaniline

*Author for Correspondence: dr.wurood.ali@gmail.com

(0.002 mol) in a NaOH solution with a pH of 5 to 6. After that, filtration, recrystallization, and drying with anhydrous calcium chloride give a green precipitate with a yield of 30% and an M.P. of 196 to 199°C, according to scheme 1.

Synthesis of metal complexes [Ni (II), Hg (II) and La (III)] with ligand (L) & curcumin

The process of creating (1:1:1) chelate complexes of the metal, curcumin and ligand (L) involved dissolving (8 mmole) L in 10 mL of absolute ethanol, which was after combined with a solution containing metal chloride salts of ($NiCl_2.6H_2O$, $LaCl_3$, and $HgCl_2$) and (8 mmole) curcumin in 20 mL of absolute ethanol. Complexes were isolated after the mix has been refluxed for a time period (3 hours) over a water bath. The finished product has undergone filtering, ethanol washing, and vacuum drying scheme 2.

RESULTS AND DISCUSSION

FTIR of the Compounds

Compound [L] has been synthesized in scheme 1 by reacting 4-aminoacetophenon, 4-methoxyanilin, and sodium nitrate in hydraulic acid. The compound [L]'s FTIR shows appearance of the bands at 1525 cm^{-1}, which are related to (N=N), and the disappearance of 2 bands of absorption at (3444 & 3194 cm^{-1}), which are related to, respectively, symmetrical and asymmetrical ($-NH_2$) group stretching (Figure 1). Some of the transition metal complexes of this ligand and curcumin are shown in the synthesis scheme, including Hg(II), Ni(II), and La(III). All complexes were synthesized by reacting compound [L] with curcumin and metal salt in ethanol (Figure 2). FTIR of complexes [Ni(cur)(L)(H2O)2]Cl, [Hg(cur)(L)(H2O) 2]Cl, [La(cur)(L)(Cl)2], Figures 3, 4 and 5) shown band shifting at 1683, 1624 cm^{-1} due to carbonyl group to higher or lower and appearance of bands at 3365, 2308 cm^{-1} which have been connected to the stretching hydroxyl group, in the end, appearance of the bands at (450–557 cm^{-1}) because of (M-N) and at (621–628 cm^{-1}) as a result of the (M-O) that confirm metal coordination with the donor atoms. Table 1 displays the compounds' FTIR spectra.[18,21]

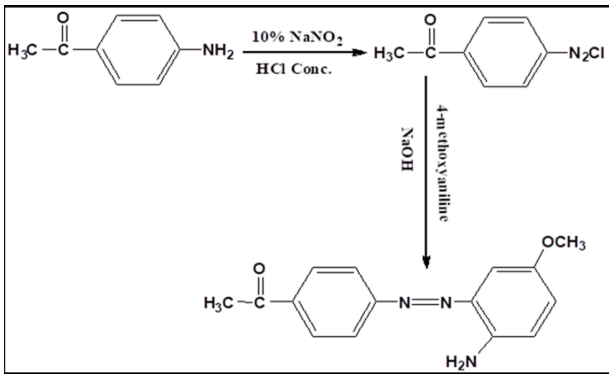

Scheme 1: Ligand (L) Synthesis

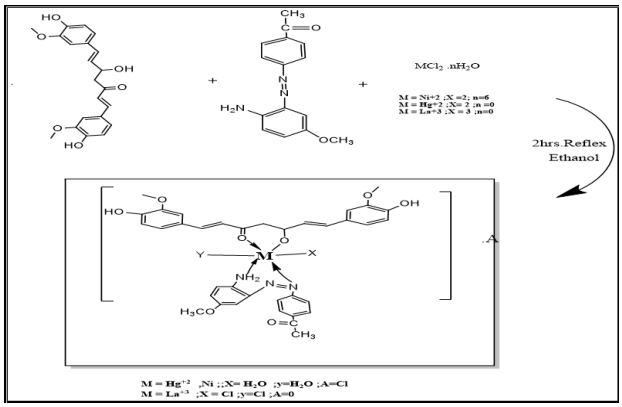

Scheme 2: Complex synthesis

Electronic Spectral Data for Complexes

UV-vis of the ligand[L] and curcumin Figures 6 and 7 spectra mainly characterized by two absorption peaks at (268, 334 nm) and (240, 304 nm) that had been assigned to (n → π*) and (π → π *), respectively. These electronic transitions were shifted

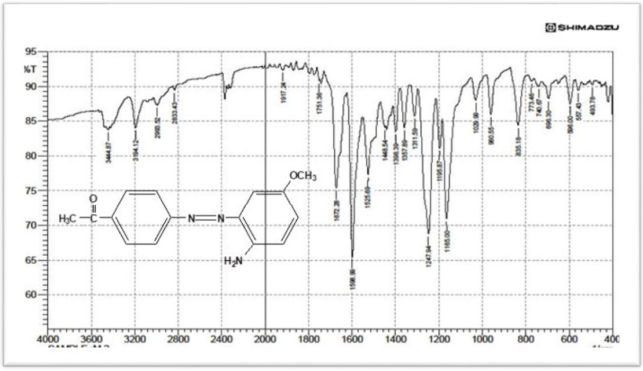

Figure 1: FTIR of ligand (L)

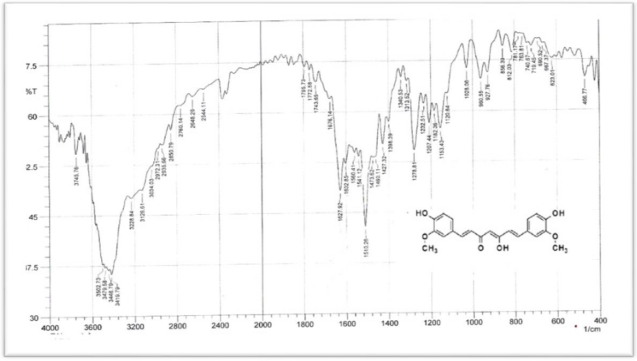

Figure 2: Curcumin FTIR

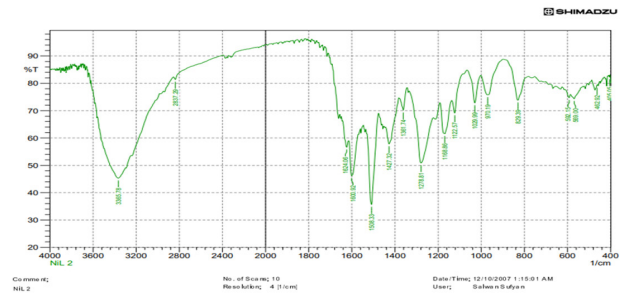

Figure 3: [Ni(cur)(L)$(H_2O)_2$]Cl FTIR

Table 1: The characteristic infra-red bands for free ligands and its metal complexes

Compound	*Colors*	*MP.*	*υ (NH2)*	*υ (O-H)*	*υ (C-O)*	*υ (N=N)*	*υ (M-N)*	*υ (M-O)*
L	Brown	201-205	34443194	------	1672	1525	--	---
Curcumin	Orange	183–185	----	3,502–3,200	1,627	----	--	--
L+ Cur.+Ni	Dark brown	>300	28372390	3365	1600	1508	462	596
L+cur.+Hg	Red-brown	>300	28352358	3365	1591	1508	474	542
L+Cur.+La	Dark yellow	>300	30002835	3390	1614	1587	453	518

Table 2: Electronic results of the conductivity as well as the compounds

Comp ound	*condu ctivity*	*λ (nm)*	*υ- (cm^{-1})*	*ε max L/mol. cm*	*Transitions*
Curcumin	-----	268	37313	530	π→π*
		334	29940	538	π→π*
		434	23041	2065	n→π*
L	-----	240	41700	1038	π→π*
		304	32900	661	n →π*
		383	26100	2306	n→π*
[Ni(cur.)(L)(H2O)2].Cl	1:1	320	31300	798	π→π*
		420	23800	879	3A2g→3 T1g(P)
		444	22500	758	3A2g→3 T1g
		686	14600	2	3A2g→3 T2g
[Hg(cur.)(L(H2O)2].Cl	1:1	319	31300	589	π→π*
		422	23700	827	Charge transfer
[La(cur.)(L)(Cl)2]0	neutral	235	42600	627	π→π*
		268	37300	455	n→π*
		400	25000	1377	Charge transfer

Table 3: Thermal analyses of [Ni(cur)(L) $(H_2O)]Cl_2$ and ligand (L)

Complex	*Stages*	*Decomposition Temperatures Initial-Final (°C)*	*Estimated (computed)*		*Assig nments*
			Mass Loss	*Total mass Loss*	
L	1	120–594.515	7.46 (7.49)	10.50 (10.51)	-(C4H4 N2O2)
[Ni(cur)(L)(H2O)2]Cl	1	100–330.148	7.88 (7.89)	5.62 (5.63)	-(C19H 18O6Cl)
	2	330.14–594.90	2.48 (2.49)		(C8H7O)

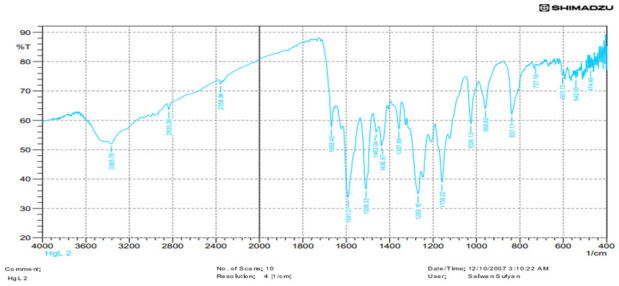

Figure 4: [Hg(cur)(L)(H2O)2]Cl FTIR

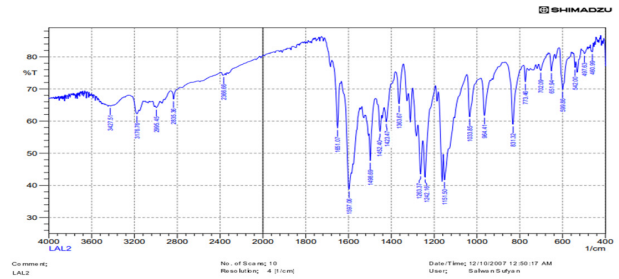

Figure 5: [La(cur)(L)Cl2] FTIR

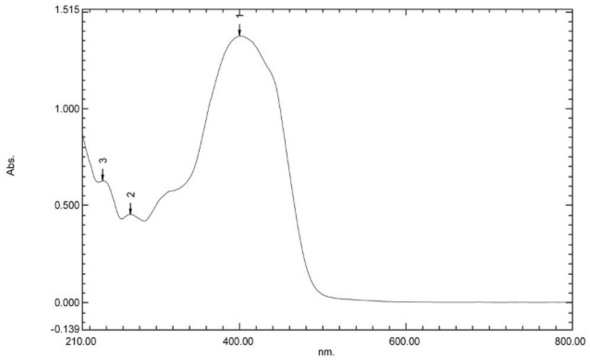

Figure 6: Electronic spectra of the ligand L

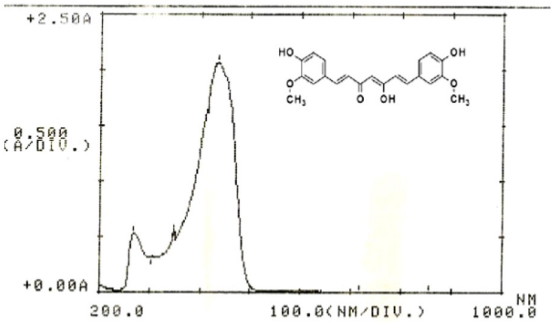

Figure 7: Electronic spectra of the Curcumin

toward lower or higher frequency values in electronic spectra of each one of the prepared complexes, ligand's coordination with metal ions are verified.

Electronic Ni (II) complex Figure 8 spectrum showed 4 new absorption peaks at (320 and 420 nm) could be given to intra ligand (Table 2). The other peak at the value (444 nm) resulted from (d-d) electronic transition type $^3A_2g \rightarrow {}^3T_1g$ while final peak at the value of (686 nm) $^3A_2g \rightarrow {}^3T_2g$. These peaks were in agreement with octa-hedral geometry for Ni (II) complex.

Hg(II) complex's electronic spectrum, as Figure 9 shows peaks of absorption at (319, 422 nm), respectively indicates ($\pi \rightarrow \pi^*$), ($n \rightarrow \pi^*$), metal ion of these complex kinds belong to the d^{10} system and that metal had not shown any (d-d) electronic transitions.

Electronic spectra of the La(III) complex Figure 10 shows peaks of absorption at 325, 268 and 400 nm indicates ($\pi \rightarrow \pi^*$), ($n \rightarrow \pi^*$) and charge transfer, respectively, metal ion of those complex types belong to d^0 system and that metal had shown no (d-d) electronic transition.[22-25]

Thermal Decomposition of $[Ni(cur)(L)(H_2O)_2]Cl$ and ligand (L)

Thermal decomposition of ligand (L)

In Figure 11, a thermo-gram for C15H15O2N3 is shown. The peak in the TGA curve at 594.515°C, which was identified, is connected to the loss of (C4H4N2O2) quantities (det. = 7.46 mg, 41.47%; calc. = 7.49 mg). C11H11N was given final portion of the compound that was seen above 594.515 (det. = 10.50, 58.36%; calc. = 10.51 mg). Peaks at 89.1, 198.9, and 309.5°C on the DSC analytical curve demonstrated a process of endothermic decomposition. Peaks at 185, 220, and 560°C have been connected to exothermic processes of decomposition.

Thermal Decomposition of $[Ni(cur)(L)(H_2O)_2]Cl$

Figure 12 depicts the thermogram for [Ni(cur)(L)(H2O)2] Cl (Table 3). The TGA curve shows a peak at 330°C that corresponds to the loss of (C19H18O6Cl) quantities (det. = 7.88 mg, 49.28%; calc. = 7.89 mg). The second step showed the loss of the (C8H7O) fragment at 594°C (obs. = 2.48 mg, 15.5%; calc. = 2.49 mg). NiC9H13O3N3 was given final portion of a compound that was noticed above 594.9 °C (det. = 5.62, 35.18%; calc. = 5.63 mg). The DSC analysis curve has demonstrated that the peaks at 109.5, 241.5, and 286.9°C indicate the endothermic decomposition process. The exothermic decomposition processes have been linked to the peaks that were seen at 205, 280, and 480°C. The exothermic argon environment. The breaking of the metal-ligand link can be seen in the final endothermic pinnacle.[26]

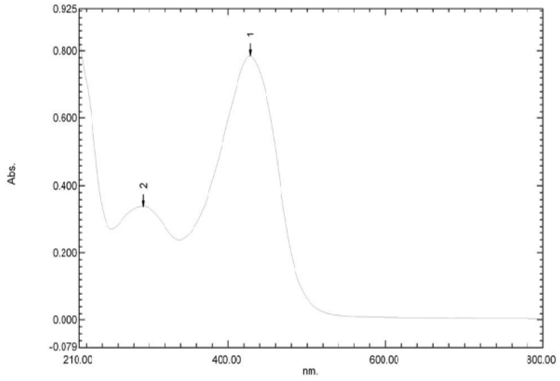

Figure 8: Electronic spectra of $[Ni(cur)(L)(H_2O)_2]Cl$

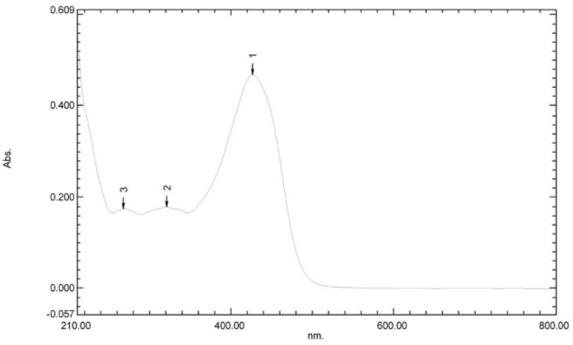

Figure 9: Electronic spectra of the $[Hg(cur)(L)(H_2O)_2]Cl$

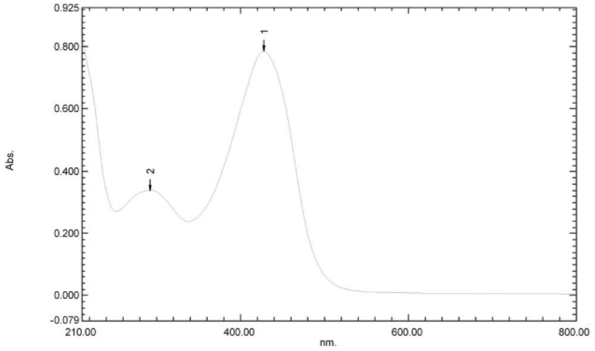

Figure 10: The electronic spectrum of [La(cur)(L)(Cl)2]

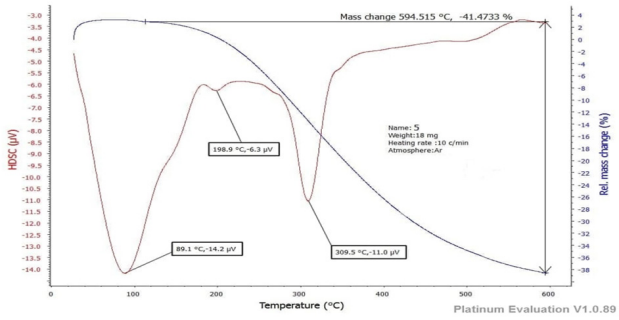

Figure 11: Thermal analysis of ligand (L)

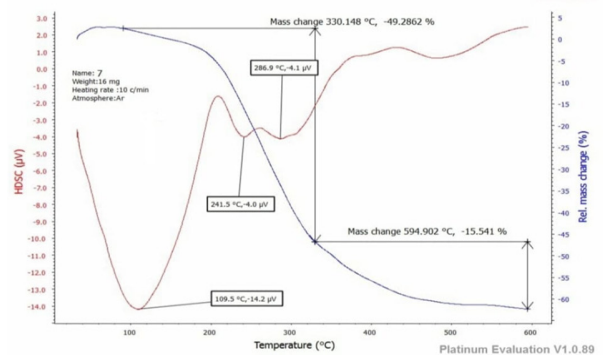

Figure 12: Thermal analyses of [Ni(cur)(L)(H2O)2]Cl

Table 4: Biological activity of synthesized compounds

Compound	*S. aureus (G+)*	*Pseudomonas (G-)*	*E. coli (G-)*	*Proteus (G-)*
Control	2	11	7	5
L	3	2	2	3
Hg-complex	17	15	7	9
Ni-complex	5	0	4	3
La-complex	8	9	4	7

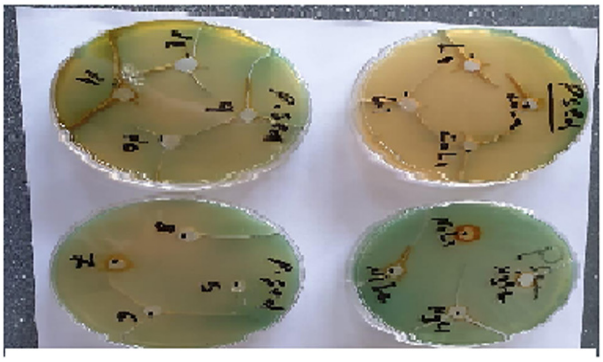

Figure 13: Biological activities of compounds

Biological screening: Test of antibacterial activities

The present study used agar diffusion method to examine the synthesized compounds' antibacterial effects against the strains of *S. aureus* (G+), *E. coli* (G), *Pseudomonas* (G-), and *Proteus* (G-). [27,28] According to the data in Table 4 and Figure 13, every compound has demonstrated biological activity against the four bacterial types after being dissolved in ethanol to produce a final (0.001 mg/mL) concentration, with the exception of Ni-complex with the *Pseudomonas*, which does not have any biological activities [zone of inhibition =0].

REFERENCES

1. Qin, J. C. and Yang, Z. Y. Bis-Schiff base as a donor–acceptor fluorescent probe: Recognition of Al^{3+} ions in near 100% aqueous solution. J. Photochem. Photobiol., A. 2015; 303-304: 99-104.
2. M.S. El-Shahawi M.S. Al-Jahdali A.S. Bashammakh A.A. Al-Sibaai H.M. Nassef "Spectroscopic and electrochemical characterization of some Schiff base metal complexes containing benzoin moiety", Spectrochimica Acta Part A: Molecular and Biomolecular Spectroscopy, 2013 113:459-465
3. Uzma Nazir, Zareen Akhter, Naveed Kausar Janjua, Muhammad Adeel Asghar, Sehrish Kanwal Tehmeena Maryum Butt, Asma Sani, Faroha Liaqat, Rizwan Hussain and Faiz Ullah Shah Biferrocenyl Schiff bases as efficient corrosion inhibitors for an aluminium alloy in HCl solution: a combined experimental and theoretical study, RSC Advances 2020, 10(13):7585- 7599
4. Ahmed Al-Amiery, Taghried A Salman, Khalida F Alazawi, Lina M Shaker, Abdul Amir H Kadhum, Mohd S Takriff. Quantum chemical elucidation on corrosion inhibition efficiency of Schiff base: DFT investigations supported by weight loss and SEM techniques International Journal of Low-Carbon Technologies 2020 15(2): 202-209.
5. Chuxin Liang Zheng Liu Qiuqun Liang Guo Cheng Han Jiaxing Han Shufen Zhang Xiao-Zhen Feng Synthesis of 2-aminofluorene bis-Schiff base and corrosion inhibition performance for carbon steel in HCl Journal of Molecular Liquids 2019, 277(1): 330-340.
6. Khan, G. Salim K. M Wan N. Basirun. J.,Mohd H. B. Faraj. L.G & Khan. M., Application of Natural Product Extracts as Green Corrosion Inhibitors for Metals & Alloys in Acid Pickling Processes - A review. Int. J.Electrochem. Sci. 2015 10: 6120 – 6134.
7. Zaki N. Kadhim Mohammed A. Mahadi Hadi Z. AlSawaad Synthesis, characterization and corrosion inhibitors Evaluation of some Schiff base complexes of Copper (II), and Molybdenum (VI) Inter. J. Acad. Stud. 2016 2(11): 446-463.
8. H. Serrar M. Larouj H.L. Gaz Z. Benzekri A. Zarguil H. Essebaai S. BoukhrisH. Oudda R. Salghi A. Hassikou and A. Souizi Experimental and Theoretical Studies of the Corrosion Inhibition of 4-amino-2-(4- chlorophenyl)-8-(2, 3-dimethoxyphenyl)-6-oxo-2, 6- dihydropyrimido [2, 1-b][1, 3] thiazine-3,7- dicarbonitrile on Carbon Steel in a 1.0 M HCl Solution Portugaliae Electrochimica Acta 2018 36(1): 35-52.
9. Y. El Kacimi M. A. Azaroual, R. Touir, M. Galai, K. Alaoui, M. Sfaira, M. Ebn Touhami and S. Kaya Corrosion inhibition studies for mild steel in 5.0 M HCl by substituted phenyltetrazole Euro-Mediterranean Journal for Environmental Integration 2017 2(1)
10. Wurood A jaafar.[2012]: IBN ALHAITHAM JORNAL, 25(1).
11. A. M. Nassar A. M. Hassan, M. A. Shoeib A. N. El kmash Synthesis, Characterization and Anticorrosion Studies of New Homobimetallic Co(II), Ni(II), Cu(II), and Zn(II) Schiff Base Complexes J Bio Tribo Corros 2015 1(19).
12. Qusay A. Jawad Dhafer S. Zinad Rawaa Dawood Salim Ahmed A Al-AmieryTayser Sumer Gaaz Mohd S. Takri_ and Abdul Amir H. Kadhum Synthesis, Characterization, and Corrosion Inhibition Potential of Novel Thiosemicarbazone on Mild Steel in Sulfuric Acid Environment Coatings 2019, 9 (729).
13. Iman Danaee S. RameshKumar M. RashvandAvei M. Vijayan Electrochemical and Quantum Chemical Studies on Corrosion Inhibition Performance of 2,2'- (2-Hydroxyethylimino)bis[N-(alphaalphadimethylphenethyl)-N-methylacetamide] on Mild Steel Corrosion in 1M HCl Solution Materials Research, 2020, 23 (2) São Carlos
14. Mustafa Alaa Mohammed, Rehab Majed KubbaExperimental Evaluation for the Inhibition of Carbon Steel Corrosion in Salt and Acid Media by New Derivative of Quinolin-2-One Iraqi Journal of Science 2020, 61(8): 1861-1873
15. Wurood A. Jaafar, Bushra M. Fayyadh, Dhuha Khudhair Rashid AL-Musawi, Basima M. Sarhan,[2022] Egyptian Journal of Chemistry, 65(13), 1527 – 1531.
16. 16. Wurood Ali Jaafar and Ruwaidah S. Saeed,[2020], Sys Rev Pharm, 11(10):134-143
17. Fayyadh, B.M., Jaafar, W.A., Sarhan, B.M.,[2021], International Journal of Drug Delivery Technology, 11(1), pp. 64–69
18. Ali M. A. Al-Khazraji, Rehab A. M. Al Hassani, Synthesis, Characterization and Spectroscopic Study of New Metal Complexes form Heterocyclic Compounds for Photostability Study Sys Rev Pharm.
19. Rehab K. al shemary, Lekaa K. Abdul Karim and Wurood A. Jaafar, [2017], Baghdad Science Journal, 14(2).
20. Kavitha, T. and Kulandaisamy, A. (2013) 'Synthesis, Spectroscopic Characterization, Electrochemical and Antimicrobial Studies of Copper(II), Nickel(II), Cobalt(II) and Zinc(II) Complexes Derived from 1-Phenyl-2,3-dimethyl-4(2-iminomethylbenzylidene)-pyrozol-5-(α-imino)-indole-3-propionic Acid', Chemical Science Transactions, 2(S1), pp. 25–32. doi: 10.7598/cst2013.3.

21. Hassan, Shaimaa A., Sajid M. Lateef, and Ismaeel Y. Majeed, Research Journal of Pharmacy and Technology 13.6 (2020): 3001-3006.
22. Hassan, Shaimaa A., Sajid M. Lateef, and Ismaeel Y. Majeed., Journal of Global Pharma Technology 10.7(2018):307-317
23. Salloom, Hawraa K., Sajid M. Lateef, and Shaimaa A. Hassan, Journal of Global Pharma Technology 12.2(2020):26-36.
24. B. S. Kusmariya, S. Tiwari, A. Tiwari, A. P. Mishra, G. A. Naiku, U. J. Pandit, J. Molec. Struct., 1116, (2016), 279–291.
25. Ali, H. S.; Khalid, F. A.; Ruwaidah S. S. Synthesis and Characterization of Some New Thiazine, Azetidine and Thiazolidine Compounds Containing 1,3,4- Thiadiazole Moiety And Their Antibacterial Study Ibn Al-Haitham Jour. for Pure & Appl. Sci. 2014,27 (3),350-364.
26. RUWAIDAH,S. S.; MUNA S. AL-R. Synthesis, Characterization, Study the Toxicity and Anticancer Activity of N,O-Chitosan Derivatives. International Journal of Pharmaceutical Research 2020, 12(2),1197-1206.
27. Fadhel, S.M; Ruwaidah, S.S; Ali, H. S. Modification and Anticancer Activity Study of Polyvinyl Alcohol Containing 1, 3, 4-thiadiazole. Journal of Global Pharma Technology2017, 10(9),345-355
28. Gao, S.; Ya, BP.; Dong, WG.; Luo, HS. "Ant proliferative effect of octreotide on gastric cancer cells mediated by inhibition of Akt/PKB and telomerase," World J. Gastroenterology 2003, 9 (10), 2362- 2365.